

»GREEN ICT @ FMD« – COMPETENCE CENTER FOR ECOLOGICALLY SUSTAINABLE ICT

Analysis of the Carbon Footprint of Self-Powered, Wireless Sensors

A Whitepaper by "HUB 1 – Sensor-Edge-Cloud-Systems"

Constantin Baumann (Fraunhofer IIS), Johannes Wieczorek (Fraunhofer IIS), Peter Spies (Fraunhofer IIS),
David Sanchez (Fraunhofer IZM)



The work presented is part of the »Green ICT @ FMD« project, your competence center for ecologically sustainable information and communication technology. The project is established by the Research Fab Microelectronics Germany and funded by the German Federal Ministry of Education and Research.

Kompetenzzentrum »Green ICT @ FMD«

c/o Forschungsfabrik Mikroelektronik Deutschland FMD
Anna-Louisa-Karsch-Str. 2
10178 Berlin, Germany

Main contact
Peter Spies peter.spies@iis.fraunhofer.de

www.greenict.de
www.forschungsfabrik-mikroelektronik.de

Date of publication
19.03.2025

Introduction

A core component of the Internet of Things are wireless sensors that collect, process and forward data from a wide variety of objects. Information is obtained from this data which is used to optimize different kinds of machines, processes and systems. In addition to increasing safety, quality, reliability and cost-effectiveness, the goal is usually also to improve sustainability. Since such sensors often have to be used and therefore produced in very large quantities, the question about their own sustainability arises.

This paper deals with the carbon footprint of the production of wireless radio sensors. A procedure is presented which estimates the carbon footprint of the production of the individual components of these wireless sensors. A wireless sensor node for measuring water, heat or electric energy consumption is used as an example. The carbon footprint of this sensor is analyzed at different power consumption values and energy supplies. The power values are resulting from varying transmission rates of the LPWAN radio module in use.

In particular, the energy supply via a primary battery and via energy harvesting from light and temperature differences is examined and the influence of run time, power requirements and environmental conditions on the carbon footprint of the different energy supplies is estimated. The ambient conditions are the usable temperature gradient for supplying the sensor using thermoelectric converters or the illuminance for generating electrical energy via solar cells. For this purpose, the battery is designed for an operating time of 10 years according to the power requirements of the sensor node and the energy harvesters are designed according to the environmental conditions and the power requirements of the sensor node. Finally, the carbon footprint of the various implementations is determined and further examined depending on the environmental conditions.

1. Energy consumption of sensor nodes in dependence of the usage profile

Wireless sensor nodes require electrical energy for their operation. To enable easy installation and use in locations without wired power supplies, this energy is typically provided by batteries. The duration until these batteries need to be recharged or replaced is significantly depending on the energy consumption of the sensor node, which in turn strongly depends on the activity and thus the usage profile of the sensor node.

Alternatively, wireless sensors can also be powered through energy harvesting from their immediate environment. Examples of such kinds of energy in the environment include light, temperature differences, deformations, or vibrations. Here, the size of the required energy harvesting system depends on the energy consumption of the sensor node and the amount of available ambient energy.

As an example, a sensor node for measuring consumption values such as heat, electrical energy or water will be considered. In **Figure 1**, the components of the considered system are shown, with yellow, blue, and orange representing the different components of the power supply options.

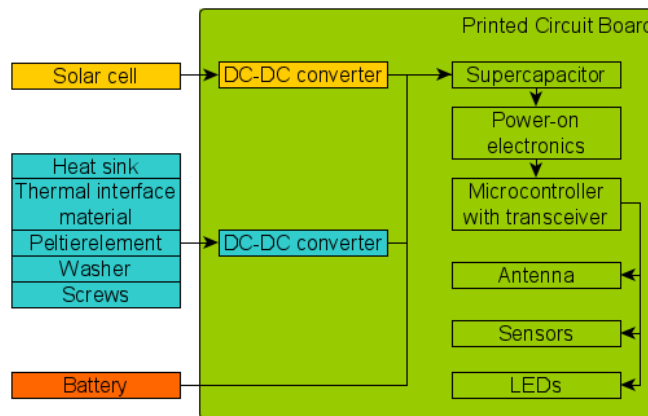


Figure 1: Components of the self-powered sensor node

The LPWAN technology mioty® is used as the radio technology in the sensor node, allowing for high transmission ranges of up to 15 km with low energy consumption. The measured values are averaged over a specific period to keep the payload and, consequently, the energy demand low. Such a radio sensor node has the power requirements listed in **Table 1**, depending on its activity. Two use cases are considered here, which differ in the interval of data transmission via radio signals.

Table 1: Parameter and power requirement of the use case

Parameter	Parameter value	
	Use case 1	Use case 2
Interval temperature measurement	16 s	16 s
Interval flow measurement	2 s	2 s
Interval radio transmission	15 min	5 min
Period of mean value calculation	60 s	32 s
Payload	61 byte	41 byte
Power requirement	400 μW	790 μW

2. Design of the Power Supply

The energy consumption of a sensor node can, for example, be covered by a battery. However, this battery must be regularly replaced or recharged depending on its capacity and the energy consumption of the sensor node. This causes maintenance efforts and therefore costs during operation, which can quickly become an economic showstopper with many installed sensors.

To keep these maintenance costs for battery replacement low, the battery should be chosen sufficiently large so that replacement is only necessary after several years. For this purpose, a lithium cell is considered here. For the selected sensor node and the presented use case 1, for example, a 34 Wh battery cell would be sufficient for about 10 years. The values can be linearly converted to other lifespan values.

To cover the energy consumption, energy harvesting technologies can alternatively be used. This eliminates the need for battery replacement, but a sufficient energy source must be available in the vicinity. For example, typical room lighting at the installation site can serve as energy source for a wireless sensor node used for consumption measurement. Optionally, a temperature difference on a supply line or pipe can also be utilized.

An example of a thermoelectric power supply is illustrated in **Figure 2**. It consists of a commercial Peltier element, a heat coupling element and a heat sink. Additionally, a voltage converter (DC-DC converter) and a capacitor are required. The presented thermoelectric energy harvester provides sufficient power to completely supply use case 1 with 400 μ W of electrical power, assuming a continuous temperature difference of 10 K between a pipe and the surrounding air with natural convection.

The thermoelectric energy harvesting system has been simulated for the use cases in COMSOL® Multiphysics. In this FEM simulation, both heat transport through natural convection and heat radiation are simulated. The simulation considers temperature differences from 0 to 70 Kelvin between the heat source and the ambient temperature. A standard aluminum pin heat sink (33 g) measuring 40x40x25 mm³ and a Peltier element measuring 12x12x4 mm³ are used. To reduce computational load, the simulation utilizes the z-x and z-y symmetry planes. The graphical model of the simulation can be seen in **Figure 2**.

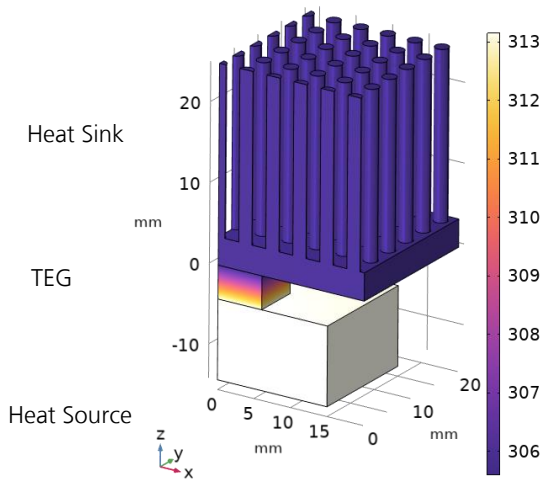


Figure 2: Simulation model in COMSOL® consisting of a heat sink, a Peltier element and a heat source

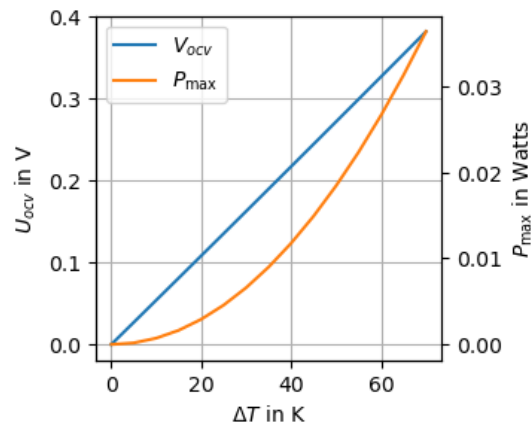


Figure 3: Open circuit voltage and maximum output power of the Peltier element over the heat source to ambient temperature difference

Figure 3 shows the simulated open-circuit voltage U_{ocv} of the thermoelectric generator as a function of the temperature difference ΔT . It also depicts the maximum electrical power P_{max} at an optimally matched load according to the formula:

$$P = \frac{U_{ocv}^2}{4R_i} \quad [1]$$

Here, R_i describes the internal resistance of the Peltier element. With a minimum temperature difference of 10 K and an efficiency of the DC-DC converter of 60%, a possible power of about 440 μ W is obtained. This power is sufficient to supply use case 1. In use case 2, two such harvesters are used.

Alternatively, solar modules can be used to power a wireless sensor node. The yield of a solar module under indoor conditions can be estimated as follows:

$$P_{max} = E_v \cdot \frac{e_r}{e_v} \cdot A \cdot \eta_{pv}(E_v) \cdot \eta_{DCDC} \quad [2]$$

Where E_v is the illumination intensity in lux, $\frac{e_r}{e_v}$ is the conversion factor from W/m^2 to lux, A is the area of the solar module, η_{pv} is the efficiency depending on the illumination intensity and η_{DCDC} is the efficiency of the DC-DC converter.

According to [1] and [2], an efficiency $\eta_{pv}(E_v)$ of 10% can be assumed at 500 lux. For the DC-DC converter, an efficiency $\eta_{DCDC} = 80\%$ can be used. The conversion factor $\frac{e_r}{e_v}$ between the illumination intensity E_v and the irradiance E_r can be estimated for the spectrum of sunlight as follows:

$$\frac{e_r}{e_v} = 0,0083 \frac{\frac{W}{m^2}}{\text{lux}} \quad [3]$$

The solar module considered in this use case has an area of 36.5 cm^2 . Thus, for 500 lux, the maximum yield from the above formula is $P_{\max} = 1,2 \text{ mW}$.

With a lighting duration of 8 hours per day, the average yield is $\bar{P} = 0.4 \text{ mW}$. Here, the losses of the energy storage are not considered. The selected solar cell thus provides sufficient power to supply use case 1 with an illumination level of 500 lux for 8 hours a day. In use case 2, two such solar cells are used to provide the required power.

3. Determination of the Carbon Footprint

To evaluate the various options for power supply in terms of their sustainability and environmental impact, the carbon footprint arising from the production of all components will be estimated and compared. In operation, these self-powered systems do not need to be powered by the grid, so their carbon footprint during operation is zero. The components of the sensor node are grouped into categories, and their share of the total carbon footprint is presented in diagrams. Component categories with a share of less than 5% are combined.

For the analysis, values from the Sphera LCA for Experts Database are used. The integrated circuits (ICs) are examined based on their packaging, meaning that the area of the dies are estimated using factors from the database. All mechanical components are analyzed based on their mass (for example, nylon spacers, thermal interface material made of boron nitride/silicone, etc.). For the heat sink, values for an anodized aluminum extrusion profile are used [3]. No further processing steps for the aluminum profile are considered. The result could be significantly reduced by using recycled aluminum. For the Peltier element (thermoelectric generator TEG), the individual components (BiTe pellets, AlO substrate, solder) are assessed and summed. For further on calculations of the carbon footprint a TEG with smaller dimensions of $9.8 \times 9.8 \times 2.1 \text{ mm}^3$ is used. This TEG has a higher power output than the TEG presented in chapter 2. This leads to a lower carbon footprint per output power and thus the carbon footprint of the thermoelectric variant is not underestimated. The manufacturing process for the mechanical components is not considered because of missing data. Therefore, due to the fact that only the single materials were considered, the carbon footprint of the components could be underestimated. The battery is considered as LiMn-CR2/3AA according to [4], and its energy content is scaled to the use cases. The assembly of the overall system and installation efforts are not considered.

The carbon footprint of the solar modules is determined based on [5]. According to this, a crystalline PV module has a carbon footprint of approximately $650 \text{ g CO}_2\text{e per watt peak}$. It is assumed that the module is produced in China and is evaluated without balance-of-system, since the electronics are assessed separately in this work.

The carbon footprint values and their distribution across the different components are obtained and the results for use case 1 are shown in **Figure 4**. Components with shares less than 5% include capacitors, resistors, inductors, supercapacitors, LEDs, crystals, transistors, antennas, screws, transformers, thermal interface materials (TIM), and in some cases, also diodes, nylon, and the TEG.

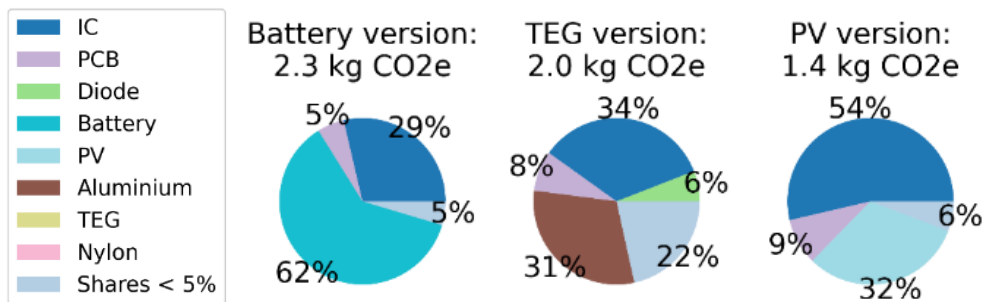


Figure 4: Carbon footprint for use case 1

In the case of the power supply with a battery, 2.3 kg CO₂e is generated for production considering a run time of 10 years. If the battery is replaced by a thermoelectric harvester, a carbon footprint of only 2.0 kg CO₂e results, which is only 87% of the carbon footprint of the battery version. With photovoltaic power supply, the carbon footprint is only 1.4 kg CO₂e, which is only 61% of the carbon footprint of the battery version. In all cases, the two largest shares of the total carbon footprint are the ICs and the power supply. In the thermoelectric variant, the shares of the ICs and the power supply (aluminum, nylon, TEG, screws, TIM) are approximately equal. In the solar variant, the ICs dominate, while in the battery variant, the power supply is predominant. The next largest influencing factor is the printed circuit board (PCB) with about 5% to 9%. All other categories have a share of less than 5% of the total carbon footprint. The size and thus the carbon footprint of the energy harvesting systems depends only on the environmental conditions and energy demand, as the environmental conditions determine the power yield for a specific size. The carbon footprint is not dependent on the lifetime, as the power is continuously supplied from the environment. In contrast, for the battery version, the carbon footprint increases with power demand and lifetime, since this also increases the size of the required battery and its carbon footprint.

For application case 2, which has approximately twice the power demand, the values for the carbon footprint are shown in Figure 5.

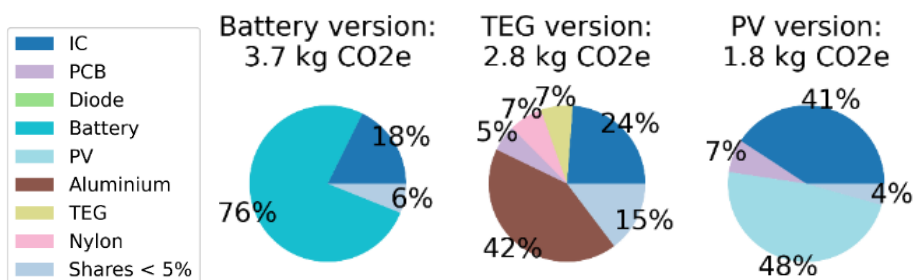


Figure 5: Carbon footprint for use case 2

In use case 2, the battery variant also has the highest carbon footprint, the thermoelectric power supply variant has a lower carbon footprint, and the solar variant has the lowest. Only the carbon footprint of the respective power supply has changed, with the battery variant increasing by a factor of about 2 and the other two variants increasing exactly by a factor of 2. The power supply has the largest share in all systems for use case 2. The total carbon footprint of the battery variant here is 3.7 kg CO₂e, which has increased by a factor of 1.61 compared to use case 1. For the thermoelectric variant, the carbon footprint is 2.8 kg CO₂e, which is only 76% of the carbon footprint of the battery variant in use case 2. It has increased by a factor of 1.40 compared to use case 1. For the solar variant, the carbon footprint is only 49% of the carbon footprint of the battery variant and has increased by a factor of 1.29 compared to use case 1. It becomes clear that in the system where the power supply has the largest share of the total carbon footprint, the overall carbon footprint increases the most when the energy demand of the use case rises. This behavior applies for a lifetime of 10 years.

Table 2: Comparison of power supply variants regarding the carbon footprint

Power supplies	(Relative) Carbon footprint		
	Use case 1 [kg CO2e]	Use case 2 [kg CO2e]	Rise from Use case 1 to Use case 2
Battery	2,3 (100%)	3,7 (100%)	1,61
Thermo-electric	2,0 (87%)	2,8 (76%)	1,40
Solar	1,4 (61%)	1,8 (49%)	1,29

4. Break-Even Point of the lifetime in the use cases and worst-case environmental conditions

At this point, the threshold at which the carbon footprint of the energy supply with a battery is higher than that of an energy supply via PV (photovoltaic) or TEG (thermoelectric generator) will be examined. For this purpose, the carbon footprint of the battery is linearly scaled with the specified lifespan of the sensor. The longer the wireless sensor is intended to be used, the larger the required battery and thus the higher the carbon footprint. However, since the energy harvesting solutions provide a constant energy yield from the environment, the carbon footprint produced during manufacturing of the energy harvesters is independent of the operational duration of the wireless sensor.

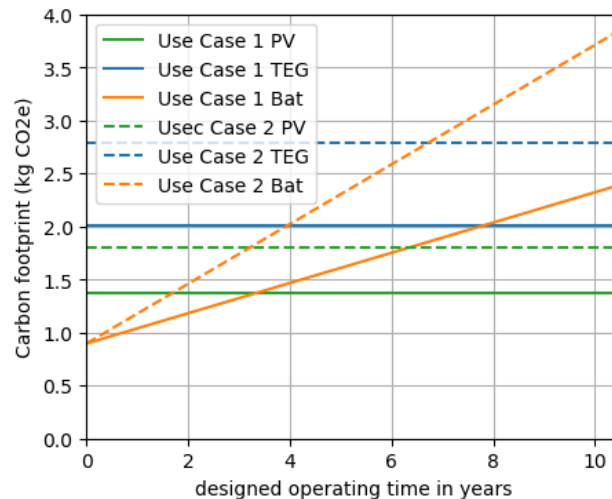


Figure 6: Carbon footprint of the use cases for each energy harvesting method compared with a battery supply

Figure 6 shows the carbon footprint of the battery solution for the two use cases as a function of the planned lifespan. At the same time, the carbon footprints of the energy harvesting solutions are plotted as constant lines, since they are independent of the planned operation time. It turns out that in the first use case, the battery-operated wireless sensor has a higher carbon footprint than the PV solution after about 3.5 years and exceeds the carbon footprint of the TEG solution after 7.5 years. The higher energy demand in the second use case causes the intersections of the carbon footprints to occur approximately half a year earlier for PV and about a year earlier for TEG. This is because, in both use cases, the PV module has a lower carbon footprint per microwatt of power than the TEG.

5. Summary

The article examines the carbon footprint of the production of wireless radio sensors. A procedure is presented that estimates the carbon footprint of the production of the individual components of these wireless sensors. The example in this article is a wireless sensor node for recording consumption values such as heat, electrical energy or water. This sensor is analyzed with regard to its carbon footprint with different power consumption values and energy supplies.

In certain scenarios, there is a lower carbon footprint in the production of the energy supply when using energy harvesting compared to operation with primary batteries. For example, it is found that with a power consumption of a wireless sensor of 800 μW and a lifespan of 10 years, the carbon footprint can be reduced by 50% if a solar cell is used instead of a primary battery, provided an illuminance of 500 lux is available for 8 hours per day. However, this carbon footprint depends on environmental conditions in the form of illuminance or temperature difference, runtime and energy requirements of the sensor node. Therefore, the intersection point at which the energy supply through energy harvesting has the same carbon footprint as supply via battery (break-even point) was examined further on.

References:

- [1] E. Bunea, K. Wilson, Y. Meydbray, M. Campbell and D. De Ceuster, "Low Light Performance of Mono-Crystalline Silicon Solar Cells," IEEE 4th World Conference on Photovoltaic Energy, Waikoloa, 2006, pp. 1312-1314.
- [2] F. Mavromatakis, F. Vignola and B. Marion, Low irradiance losses of photovoltaic modules, Solar Energy, 2017, pp. 496-506.
- [3] S. Benecke, "Systemverhalten von Energy Harvestern in autonomen Sensoren unter Betrachtung der Wechselwirkung von Funktionalität und Umweltverträglichkeit", Ph.D. Dissertation, Technische Universität Berlin, 2019
- [4] E. Masanet and A. Horvath, "Battery Case Study: The Impact of Extended Producer Responsibility in California on Global Greenhouse Gas Emissions." <https://www2.calrecycle.ca.gov/Publications/Download/1002>, 2012.
- [5] A. Khan et al., "Global warming potential of photovoltaics with state-of-the art silicon solar cells: Influence of electricity mix, installation location and lifetime", Solar Energy Materials and Solar Cells, 2024.
- [6] P. R. Michael, D. E. Johnston and W. Moreno, "A conversion guide: solar irradiance and lux illuminance," Journal of Measurements in Engineering, vol. 8, no. 4, pp. 153–166, Dec. 2020, doi: 10.21595/jme.2020.21667.